THE JOURNAL OF PHYSICAL CHEMISTRY B

ARTICLE

pubs.acs.org/JPCB

Dielectric Dependence of the First Molecular Hyperpolarizability for Electro-Optic Chromophores

Denise H. Bale, Bruce E. Eichinger, Wenkel Liang, Xiaosong Li, Larry R. Dalton, Bruce H. Robinson,* and Philip J. Reid*

Department of Chemistry, University of Washington, P.O. Box 351700, Seattle, Washington 98195, United States

Supporting Information

ABSTRACT: Experimental and computational studies of the solvent dependence of the first molecular hyperpolarizability (β) for two donor-bridge-acceptor chromophores (CLD-1 and YLD156) are presented. Hyper-Rayleigh scattering (HRS) measurements are performed with 1907 nm excitation in a series of solvents with dielectric constants ranging from ~2 (toluene) to ~36 (acetonitrile). For both chromophores an approximately 2-fold increase in β is observed by HRS over this range of dielectric constants. Computational studies employing a polarized continuum model to represent the solvent are capable of reproducing this experimental result. The experimental and computational results are compared to the predictions of the widely employed two-state model (TSM) for β. Surprisingly, for the chromophores studied here the TSM predicts that β should *decrease* with increasing dielectric constant over the range investigated. The results presented here demonstrate that the TSM provides neither a quantitative nor qualitative description of the solvent dependence of β for CLD-1 and YLD156. The enhancement of β with increased dielectric constant suggests that modification of the dielectric surrounding the chromophore is one path by which the performance of nonlinear optical devices employing these chromophores may be significantly enhanced.

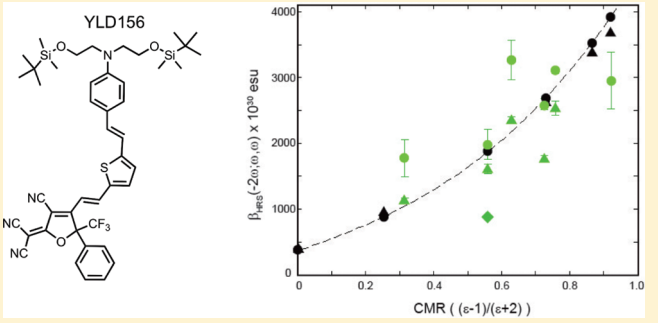

INTRODUCTION

The development of organic materials for nonlinear optical (NLO) applications has been an active field of research since the early 1970s.[1] Recently, remarkable progress has been made in enhancing the performance of these materials, leading to significant advances in telecommunications and other optical-switching applications.[2−4] The interest in organic materials for NLO devices is well-justified since these materials can be used to manufacture low-cost, low-power-consumption devices, and can be synthetically altered to improve their performance as opposed to existing, widely deployed inorganic materials. For example, lithium niobate ($LiNO_3$) is widely employed in NLO devices such as electro-optical (EO) switches; however, this material has a modest EO coefficient (r_{33} = 30.9 pm/V) and incorporation of this material into devices is nontrivial. Recently organic materials have demonstrated r_{33} values that are more than 10 times that of $LiNO_3$, and can be easily processed from solution simplifying incorporation into various device structures.[2,5−7] In short, future advances in optical-switching technologies will most likely involve organic NLO materials.

In addition to advances in material performance, knowledge of the basic operational and design principles of organic NLO materials has increased significantly over the past decade.[3,8] For example, we recently reported on a mixed quantum mechanical/statistical mechanical study in which the EO properties of a composite material were reproduced using quantum-mechanical calculations of chromophore properties with statistical−mechanical determination of chromophore interactions in the material.[8] One issue that emerged in this study was the extent to which computationally determined chromophore properties such as the first molecular hyperpolarizability (β) are maintained in a complex media. For example, in chromophore/polymer composite materials the chromophore can be present at concentrations up to 20% by weight. At these elevated concentrations, the contribution of neighboring chromophores to the dielectric environment provided by the polymer host may significantly perturb β. Current interest in this area involves understanding the influence of the surrounding dielectric on molecular NLO properties.

The effect of dielectric on linear molecular optical properties is a well-studied field. For example, the solvatochromatic behavior of electronic absorption bands has been studied for roughly 50 years.[9] In comparison, the study of solvent effects on molecular NLO properties is relatively new. Roughly a dozen experimental studies involving the solvent-dependence of molecular hyperpolarizabilities have been performed to date.[10−22] The pioneering work of Marder and co-workers provided an initial description of

Received: October 14, 2010
Revised: February 24, 2011
Published: March 16, 2011

the interplay between β and the dielectric properties of the solvent.[10−14,22] In this description, the solvent dependence of β for electron donor-bridge-acceptor chromophores (also referred to as "push-pull" chromophores) arises from changes in bond-length alternation (BLA) of the conjugated bridge connecting the donor and acceptor with a change in solvent. As the polarity of the solvent is increased, the structure of the chromophore evolves from neutral (BLA > 0) to cyanine-like (BLA = 0) to zwitterionic (BLA < 0). The connection between β and BLA was cast in terms of the two-state model (TSM) where $\beta \propto (\mu_{ee} - \mu_{gg})(\mu_{ge}^2)(\Delta E_{ge}^2)^{-1}$.[12,23,24] The first term in this expression is the difference in permanent dipole moment between the excited and ground electronic states, μ_{ge} is the transition dipole moment connecting the ground and excited state, and ΔE_{ge} is the difference in energy between the ground and excited states. The TSM depicts β as being dependent on three parameters, all of which may be solvent dependent. Subsequent studies have explored the validity of the TSM in describing the solvent-dependence of β, with qualitative utility of this model being demonstrated for numerous systems.[12,15,19,20] Computational studies have also found the TSM to be a reasonable description of β solvent-dependence.[25−29] There are three notable exceptions to these studies. First, resonance Raman studies of azulenic-thiobarbituric acid donor−acceptor chromophores demonstrated that the TSM does not accurately describe these materials since more than a single excited state contributes to β.[21] Second, computational studies of a series of merocyanine compounds demonstrated poor quantitative agreement with the TSM.[30] Finally, studies of modified DANS found that the HRS intensity measured with excitation two-photon resonant with the lowest-energy electronic transition was greater than could be accounted for assuming the scattering originates from this lowest-energy state exclusively, suggesting that the contributions from nonresonant electronic states was substantial.[18]

In this paper, we present a combined experimental and computational study of the solvent dependence of β for two modern donor-bridge-acceptor chromophores: CLD-1 and YLD156 (Scheme 1). These chromophores consist of a substituted-amine donor and a tricyanofuran acceptor connected by a conjugated bridge. Hyper-Rayleigh scattering (HRS) measurements are performed with 1907 nm excitation in a variety of solvents spanning a range of dielectric constants from $\varepsilon \approx 2$ (toluene) to $\varepsilon \approx 36$ (acetonitrile). For both chromophores, a 2-fold increase in β occurs with an increase in dielectric constant over this range. Computational studies are performed employing polarized continuum models to represent the solvent, and these studies are capable of reproducing the increase in β. The experimental and computational results are compared to the predictions of the TSM. Surprisingly, for the chromophores studied here the prediction of the TSM is that β should *decrease* over the range of dielectric constants investigated. Furthermore, the BLA values for these chromophores approach zero as the solvent polarity increases, consistent with the prediction of the TSM of reduced β. In short, the results presented here demonstrate that the TSM provides neither a quantitative nor qualitative description of the solvent dependence of β for CLD-1 and YLD156. These results also demonstrate the need to consider more than a single excited state when determining the value of β in complex environments. Finally, significant enhancement in β with increased dielectric suggests that modification of the dielectric surrounding the chromophore may be a way to significantly enhance NLO device performance.

EXPERIMENTAL SECTION

Synthesis. Molecular structures of the chromophores studied here are presented in Scheme 1. The synthesis of YLD156 [2-[4-(2-{5-[2-(4-{Bis-[2-(*tert*-butyl-dimethyl-silanyloxy)-ethyl]-amino}-phenyl)-vinyl]-thiophen-2-yl}-vinyl)-3-cyano-5-phenyl-5-trifluoromethyl-5H-furan-2-ylidene]-malononitrile] and CLD-1 [3-Cyano-2-dicyanomethylidene-4-{*trans,trans,trans*-[3-(2-(*p*-*N*,*N*-bis(2-*tert*-butyldimethylsiloxyethyl)aminophenyl)vinyl)cyclohex-2-enylidene]-1-propenyl}-5,5-dimethyl-2,5-dihydrofuran] have been reported previously.[31,32] Solutions prepared for HRS studies were kept at low concentration ($\leq$100 μM) to minimize self-absorption of the scattered radiation. HRS data were collected on YLD156 and CLD-1 in a variety of solvents: chloroform (CFM, Fisher ACS Spectranalyzed), dichloromethane (DCM, dispensed from a solvent purification system using two alumina columns), 1,2-dichloroethane (DCE, Alfa Aesar, 99+%), ethyl acetate (EA, fractionally distilled from and onto 4 Å molecular sieves), acetonitrile (MeCN, fractionally distilled from and onto

Scheme 1. Molecular Structures of the Chromophores Used in This Study[a]

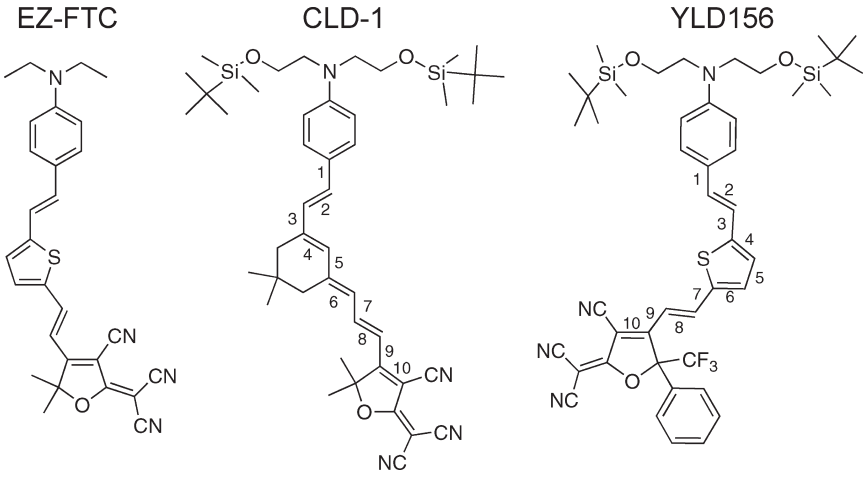

[a] EZ-FTC, CLD-1, and YLD156. Bond labels employed in the bond-length alternation theoretical analysis are shown for CLD-1 and YLD156.

4 Å molecular sieves), and toluene (TOL, dispensed from a solvent purification system using two alumina columns).

Theoretical Methods. Of interest here is the comparison between the β determined using HRS and that predicted from theory. The β derived from the perturbation expansion (as opposed to a Taylor series expansion) of the molecular polarization in terms of the applied electric field F is given by

$$\langle \mu_i \rangle = \mu_i + \alpha_{ij}F_j + \beta_{ijk}F_kF_j + \ldots \tag{1.1}$$

where summation notation over the $\{i,j,k\}$ indices is implied.[33] Quantum-mechanical codes compute the energy (E) of the system, which can be connected to the polarization. When the electric field is the dominant perturbation, the perturbation part of the Hamiltonian in the zero-frequency limit of the light fields, F, becomes

$$\hat{H}^1 = -F_i\hat{\mu}_i \tag{1.2}$$

Using the Hellman−Feynman theorem, the energy of the system and the dipolar expectation values are related by

$$\langle \mu_i \rangle = -\frac{dE}{dF_i} \tag{1.3}$$

The energy expressed as an expansion in powers of the perturbation, $\hat{H}^1$, is given by:

$$E = E_o + E_1 + E_2 + E_3 \ldots \tag{1.4}$$

From eq 1.4, the various orders of the expansion can be determined as a sum over states using the unperturbed wave functions as a basis set for that expansion. In particular, the third-order correction to the unperturbed energy is

$$E_3 = -\sum_{\{i,j,k\}} F_i \sum_e \sum_{e'} \frac{\mu^i_{0,e}[F_j \cdot (\mu^j_{e,e'} - \mu^j_{0,0}\delta_{e,e'})]\mu^k_{e',0}}{(\varepsilon_e - \varepsilon_0)(\varepsilon_{e'} - \varepsilon_0)}F_k \tag{1.5}$$

where the sum over $\{i,j,k\}$ is implied and the sum over all excited states $\{e,e'\}$ is explicitly given. The ground state energy, E_o=ε_o, is not included in the sum over molecular states. Using the Hellman−Feynman theorem each order of the energy expansion can be equated to the appropriate derivatives of the dipolar expectation values:

$$\left.\frac{d^2\langle \mu_i \rangle}{dF_j dF_k}\right|_{F=0} = -\frac{d^3E_3}{dF_i\, dF_j\, dF_k} = 2\beta_{ijk} \tag{1.6}$$

Using the above expression, eqs 1.1, 1.5 and 1.6, the β tensor elements can be written in terms of the unperturbed dipolar components as

$$\beta_{ijk} = \frac{1}{2}\sum_{P\{i,j,k\}} \sum_e \sum_{e'} \frac{\mu^i_{0,e}[(\mu^j_{e,e'} - \mu^j_{0,0}\delta_{e,e'})]\mu^k_{e',0}}{(\varepsilon_e - \varepsilon_0)(\varepsilon_{e'} - \varepsilon_0)} \tag{1.7}$$

In eq 1.7 the sum over all six permutations of the $P\{i,j,k\}$ indices is required. In particular, the zzz element of the β tensor can be written as

$$\beta_{zzz} = 3\sum_e \sum_{e'} \frac{\mu^z_{0,e}(\mu^z_{e,e'} - \mu^z_{0,0}\delta_{e,e'})\mu^z_{e',0}}{(\varepsilon_e - \varepsilon_0)(\varepsilon_{e'} - \varepsilon_0)} \tag{1.8}$$

For the "push−pull" chromophores of interest in this study, β_{zzz} is the dominant tensor component; however, averaging over all tensor elements was performed to calculated β_{HRS}. This derivation of the β tensor elements is for the case where the light fields, F_j, are time independent. The comparable development of the β tensor using time dependent perturbation fields is more complicated but retains many of the features of this result.

We now focus on the components of β that are particularly applicable to the HRS experiment, in which the second harmonic signal 2ω is generated from an initial light field at frequency ω. The β elements relevant to this type of experiment are described as $\beta_{ijk}(-2\omega;\omega,\omega)$. The dominant element tensor (and main contributor to the HRS signal) is the $\beta_{ijk}(-2\omega;\omega,\omega)$ given by the sum-overstates model as

$$\beta_{zzz}(-2\omega;\omega,\omega) = 3\sum_e \sum_{e'} \mu^z_{0,e}[(\mu^z_{e,e'} - \mu^z_{0,0}\delta_{e,e'})]\mu^z_{e',0}D_{e,e'}(\omega,\gamma) \tag{1.9}$$

Here, the energy term in the denominator in eq 1.7 is replaced by a more complicated term, $D_{e,e'}(\omega,\gamma)$, that includes the frequency of the incident light field, ω, as well as an ad hoc line width parameter, γ, which accounts for resonance and dispersion effects.[34−36]

$$D_{e,e'}(\omega,\gamma) = \frac{1}{3}\left\{\frac{1}{(\Omega_e - 2\omega)(\Omega_{e'} - \omega)} + \frac{1}{(\Omega^*_e + \omega)(\Omega_{e'} - \omega)} + \frac{1}{(\Omega^*_e + \omega)(\Omega^*_{e'} + 2\omega)}\right\},$$
$$\text{where } \Omega_e = \varepsilon_e - \varepsilon_0 - i\gamma \tag{1.10}$$

This term reduces to the previous expression of eq 1.8, when ω and γ are set to zero:

$$D_{e,e'}(0,0) = \frac{1}{(\varepsilon_e - \varepsilon_0)(\varepsilon_{e'} - \varepsilon_0)} \tag{1.11}$$

Computationally, the sum-over-states formulas are not used to compute the elements of the β tensor.[37,38] Rather, finite field formulas are applied to extract the tensor elements from changes in energy using the perturbation expression for the dipolar expectation values, eqs 1.1 and 1.6, which follows from the Hellman−Feynman theorem, eq 1.3. An additional minor point is that the Gaussian[37] computational suite employs a Taylor-series expansion; therefore, β values obtained from these calculations must be divided by 2 to be the same as the tensor elements defined in eq 1.1.[33]

In the standard two-state model (TSM) only the lowest energy excited state (e) is retained in the expression for β, thus yielding

$$\beta^{TSM}_{ijk}(-2\omega;\omega,\omega) = \frac{1}{2}\sum_{P\{i,j,k\}} (\mu^i_{0,e}\mu^k_{e,0})(\mu^j_{e,e} - \mu^j_{0,0})D_{e,e}(\omega,\gamma) \tag{1.12}$$

The sum over all permutations of $\{i,j,k\}$ is implied and $D_{e,e}(\omega,\gamma) = D_{1,1}(\omega,\gamma)$ is evaluated at the first excited state. Again the most important element in the TSM (for the HRS experiment) is the zzz element:

$$\beta^{TSM}_{zzz}(-2\omega;\omega,\omega) = 3(\mu^z_{0,e}\mu^z_{e,0})(\mu^z_{e,e} - \mu^z_{0,0})D_{1,1}(\omega,\gamma) \tag{1.13}$$

dx.doi.org/10.1021/jp109870y |J. Phys. Chem. B 2011, 115, 3505–3513

The TSM expression (eq 1.12) shows that the inclusion of both a line width effect and the dependence upon the frequency of the light can be included to obtain a relation between the β at any frequency and the frequency independent limit:

$$\beta_{ijk}^{TSM}(-2\omega;\omega,\omega) = \beta_{ijk}^{TSM}(0;0,0)\cdot K_D(\omega,\gamma),$$
$$\text{where } K_D(\omega,\gamma) = \frac{D_{1,1}(\omega,\gamma)}{D_{1,1}(0,0)} \quad (1.14)$$

Notice that within the TSM, knowledge of the solvent dependence of the ground and excited-state dipole moments, the transition dipole moment coupling the ground and excited states, and the ground−excited state energy gap are all that is required to predict the variation of β with any other parameter (including solvent). The ability of the TSM to reproduce the solvent dependence of measured β will be explored below. The TSM suggests the following relationship between a full calculation of β at the frequency of interest and the frequency independent limit:

$$\beta_{ijk}(-2\omega;\omega,\omega) \approx \beta_{ijk}(0;0,0)\cdot K_D(\omega,0) \quad (1.15)$$

This assumption has been used in previous work[8,39] and will be examined below.

Two issues must be addressed when comparing theoretical values of β to HRS data. First, the β determined by HRS corresponds to the average over all β tensor elements for a uniform molecular orientation distribution in solution.[40] The averaging is performed as shown:

$$(\beta_{HRS}(-2\omega;\omega,\omega))^2 = \sum c_{ijk}^{i'j'k'}\beta_{ijk}(-2\omega;\omega,\omega)\beta_{i'j'k'}(-2\omega;\omega,\omega) \quad (1.16)$$

The coefficients were determined by Cyvin et al.[40] based on a uniform orientation distribution. Second, HRS measurements are performed at a specific frequency; therefore, linewidths for the electronic transitions of interest and the corresponding frequency dependence of HRS intensities must be considered. The line width (and its contribution to the dispersion effect) is not part of any standard calculation package and may partially play in missing important additional features in spectral fitting. At present then, we can only use a ratio method to estimate the effects of line width on the estimates of β by assuming

$$\beta_{ijk}^{\gamma}(-2\omega;\omega,\omega) \approx \beta_{ijk}^{\gamma=0}(-2\omega;\omega,\omega)\cdot\frac{D(\omega,\gamma)}{D(\omega,0)}$$
$$\beta_{ijk}^{0}(-2\omega;\omega,\omega) \approx \beta_{HRS}^{0}(-2\omega;\omega,\omega)\cdot\left|\frac{D(\omega,\gamma)}{D(\omega,0)}\right| \quad (1.17)$$

Computational Methods. The molecular properties of the chromophores studied here were calculated using the density functional theory (DFT) methodology in Gaussian03 or Gaussian09.[37] In all cases the B3LYP functional with the 6-31G* basis set was used for geometry optimizations as well as property evaluation. The model compound used for calculations was a single conformation of the *N*,*N*-dimethyl version of the chromophores. Properties were surveyed using a few different computational protocols so as to explore a limited range of basis sets (3-31G* and 6-21G*), reaction field effects (PCM (polarized continuum model) and COSMO), and geometric constraints. Calculations were also done with DMol using the PBE functional with the numerical DNP basis set and COSMO reaction field model.[37,38] The larger basis set made only a small change in the solvent dependent hyperpolarizabilities.

In one series of calculations the 3-21G* basis set was used to optimize the molecular geometry followed by solvent polarity calculations with the PCM option. The latter were done on a fixed molecular geometry using a numerical range of solvent radii (2.0−4.0 Å) and dielectric constants (2.0−16.0). For a fixed dielectric constant of 4.0, solvent radii of 2.0, 3.0, and 4.0 gave $\beta_{HRS}/10^{-30}$ esu ranging from 506 to 499 to 495, respectively. This small variation was judged to be insignificant; therefore all subsequent calculations in this series were done with the solvent radius fixed at 3.0 Å. The PBE/DNP/COSMO calculations were done with a solvent radius of 1.5 Å using fields with strength 0.0005 au and 0.001 au aligned along the three axes of an arbitrarily rotated Cartesian frame. Each predicted β_{HRS} value was determined from the complete set of tensor elements appropriately averaged using the procedure of Cyvin et al.[40] In summary, the variation of properties with dielectric constant are consistent between the PCM and COSMO methods using the same functional, with quantitative differences between them ranging ca. 17% for the dipole moments with a dielectric constant of 8.0 and only 0.2% for β_{zzz} of the same dielectric. As observed previously, hyperpolarizabilities are less sensitive to functional and basis set than dipole moments.[41]

A direct comparison between experimentally determined HRS hyperpolarizabilities and those predicted from theory can be made that include both the effects of solvent and the frequency of the light field. In this computational approach, the polarization of the solvent surrounding a polar solute molecule generates a reaction field that acts back on the solute. If the bare dipole moment of the solute is large, the reaction field becomes sufficiently large to perturb the molecular β. Computational methods, such as COSMO in DMol and the polarizable continuum model (PCM) in Gaussian, have provided reasonable approximations of electrostatic solvent effects.[8] These theories are based on distribution of charge over a molecular surface as opposed to a dielectric continuum, and allow for the inclusion of inhomogeneous reaction field effects resulting from the atomistic solvent environment.[37,38]

HRS Methods. Electronic absorption spectra of YLD156 and CLD-1 were obtained using a UV−vis spectrometer (Shimadzu UV-1601). HRS studies were performed using the output of a Q-switched Nd:YAG laser (Spectra-Physics GCR-170) operating at 1064 nm with a repetition rate of 30 Hz. The laser output was delivered to a 1-m long Raman-shifting cell filled with H_2 at a pressure of ~20 atm. The first Stokes line at 1907 nm (5244 cm^{-1}) was isolated using a Pellin-Broca prism, dichroic mirrors and a Corning long-pass emission filter (CS 2−64) resulting in an incident power of 400 mW. A 90-degree scattering geometry was employed. A 300 mm f.l. plano-convex lens was used to focus the 1907 nm beam into a low-volume flow cell having a 10 mm path length along the direction of the incident field, and a 2 mm path lenght along the direction of the collection optics. The beam waste of the incident field was positioned toward the top of the cell such that the collected scattered volume is at the end of the 10 mm flow cell. Photodegradation of the sample was minimized by circulating the sample with a peristaltic pump equipped with Viton or PTFE tubing and an inline 0.2-μm filter to remove particulate matter. Scattered light at 953.5 nm was collected with standard refractive optics and delivered to a 0.75-m

focal length monochromator (Acton) equipped with a 1200 grooves mm^{-1} classically ruled grating (λ_{blaze} = 500 nm). A 950 nm interference filter (40 nm fwhm) was positioned in front of the monochromator entrance. Detection was accomplished using a red-edge enhanced, back-thinned, liquid-nitrogen-cooled CCD camera (Princeton Instruments, Roper Scientific Spec-10: 100BR) with exposure times of 240−540 s. HRS intensities were determined to increase as the square of the incident power and linearly with concentration. The measured scattered light was fit to a Gaussian function with HRS intensities reported here corresponding to the area of the fitted curve as described elsewhere.[42]

Molecular hyperpolarizabilities were derived from the HRS data using the external-reference method. In this approach, the HRS intensity from the sample is measured and compared with that of a standard. That standard employed for these measurements was the chromophore EZ-FTC (Scheme 1) dissolved in chloroform, which is the only solvent used for the reference. In this approach, β_{HRS} determined for the molecule of interest in any of a variety of solvents relative to the standard is given by:

$$\beta_{rel}^{mol/sol}(-2\omega;\omega,\omega) = \frac{\beta_{HRS}^{mol/sol}(-2\omega;\omega,\omega)}{\beta_{HRS}^{FTC/CHCl_3}(-2\omega;\omega,\omega)} = \left[\frac{I_{molec}(2\omega)}{I_{FTC}(2\omega)}\frac{N_{FTC}}{N_{molec}}\right]^{1/2} \quad (1.18)$$

In the above expression, β_{HRS} is the orientationally averaged first molecular hyperpolarizability, N is the number density of chromophore in solvent, and $I(2\omega)$ is the measured HRS intensity. The solvents investigated here have a transmission factor $T(\omega)$ ranging from 0.74 to 0.19 at 1.9 μm corresponding to the change in incident field intensity with propagation through the flow cell; therefore, the effect of reduced transmission was accounted for using $I(2\omega) \propto \langle\beta_{rel}^{mol/sol}\rangle(T(\omega)^2)$, where the transmittance of chloroform is unity at 1907 nm, and thus does not appear in this expression. Reported values correspond to the average of three to four measurements and errors correspond to 1 standard deviation from the mean of these measurements.

RESULTS

HRS Results. Figure 1 presents the absorption spectra of YLD156 and CLD-1 in solvents of interest for this study. Absorption spectra were acquired for YLD156 and CLD-1 in solvents with concentrations ranging from 5 to 100 μM, and the width of the absorption spectrum was found to be independent of concentration consistent with the absence of aggregation over this range of concentrations. Because of limited solubility, the spectrum of CLD-1 in acetonitrile could not be measured. The wavelengths of each absorbance maximum are shown in Figure 2 and available in tabulated form in the Supporting Information. Also shown in Figure 2 are the calculated values for the band gap transition energies, ΔE, determined from time-dependent density functional theory (TD-DFT) as describe above. The figure illustrates that theory consistently underestimates the experimental band gap for CLD-1 and overestimates the band gap for YLD156. Figures 1 and 2 illustrate that the absorption maximum for CLD-1 is at higher energy relative to YLD156 for a given solvent. For both compounds, the absorbance maximum in ethyl acetate appears to be anomalously blue-shifted. In Figure 2 (and subsequent figures), the abscissa is plotted in terms of the

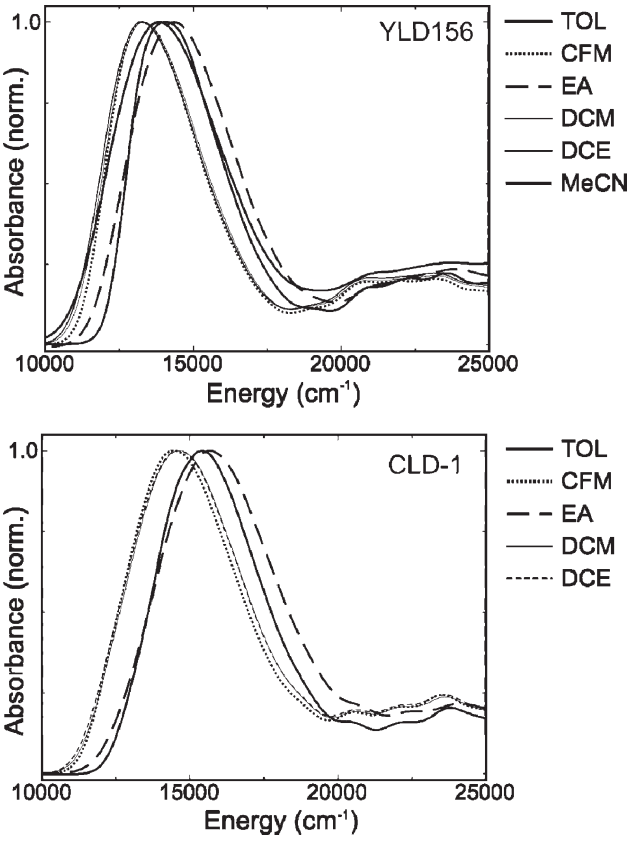

Figure 1. Normalized absorption spectra of YLD156 (top) and CLD-1 (bottom) as a function of solvent: toluene (TOL), chloroform (CFM), ethyl acetate (EA), dichloromethane (DCM), 1,2-dichloroethane (DCE), and acetonitrile (MeCN).

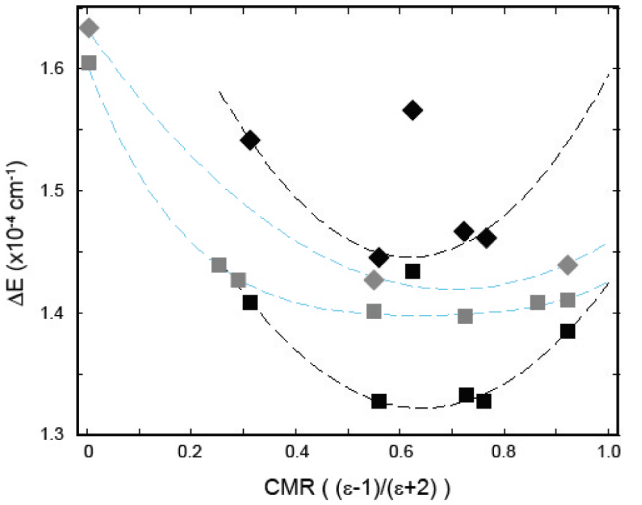

Figure 2. Measured (black) and predicted (blue) transition energies of YLD156 (squares) and CLD-1 (diamonds) as a function of solvent. Predicted ΔE values are obtained from the LUMO and HOMO energies; the experimental values are obtained from the maximum absorption (Figure 1). The dashed lines are least-squares best fits to the data using 4th order polynomial, and are provided solely to guide the eye. The experimental data of ethyl acetate (points at *cmr* = 0.63) are not included in the fits.

Classius Mossotti ratio, *cmr*, which is a function of the relative dielectric ε of the different solvents given by $cmr = (\varepsilon - 1)/(\varepsilon + 2)$.

dx.doi.org/10.1021/jp109870y |J. Phys. Chem. B 2011, 115, 3505–3513

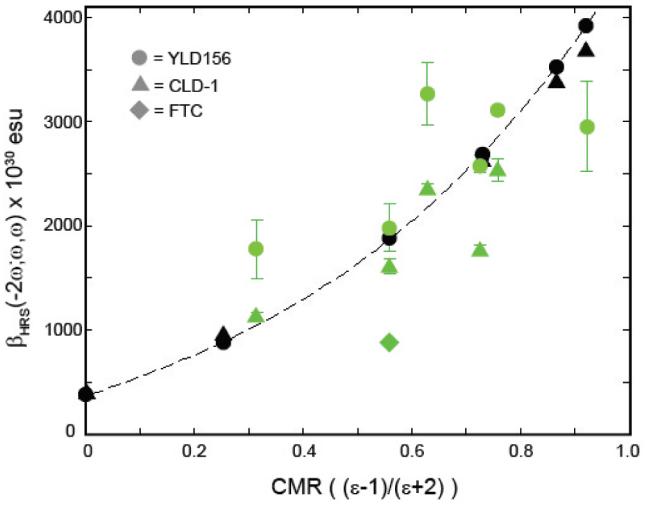

Figure 3. Comparison of measured and predicted $\beta^{\varepsilon}_{HRS}(-2\omega;\omega,\omega)$ values as a function of solvent. Experimental data are presented as green symbols, and theoretical predictions as black symbols. The dashed line is simply a trend line (as a least-squares quadratic polynomial fit to the theory for YLD156) connecting the theoretical values.

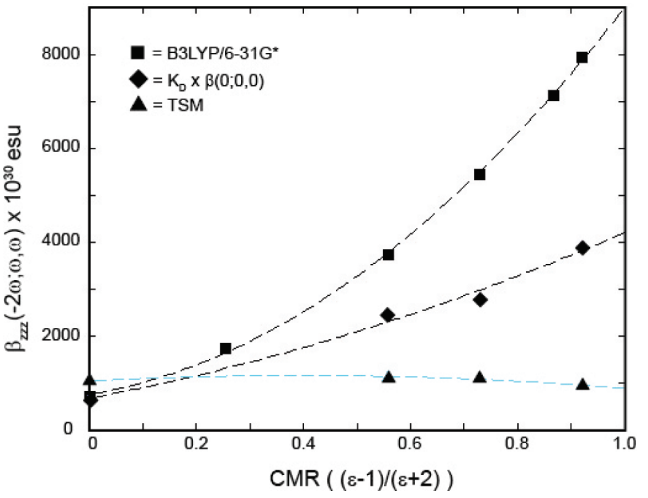

Figure 4. Comparison of theoretical methods used for predicting $\beta^{\varepsilon}_{zzz}(-2\omega;\omega,\omega)$ including frequency and dielectric with two different approximations. All computations were done on geometry-optimized structures at each dielectric. All spectra were computed at 1907 nm (5244 cm^{-1}). The prediction of the TSM is shown in green using eq 1.12. The approximation of eq 1.15 is also compared to the full calculation. This shows the effect of just using the dispersion frequency term $K_D(\omega,\gamma)$ on β at zero frequency. In this example $\gamma = 0$. The dashed lines are second-order least-squares fit polynomials of the *cmr*, and are merely to aid the eye.

The *cmr* has the effect of compressing the dielectric-scale from 0 to 1 rather than from 1 to infinity, and the use of this ratio is somewhat justified in that the theoretical β for the molecules of interest varies nearly linear with this parameter.[8]

The values of $\beta^{mol/sol}_{rel}$ for YLD156 and CLD-1 as a function of solvent were measured employing excitation at 1907 nm. These experimental, relative values were multiplied by a factor of 890 × 10^{-30} esu to provide optimal agreement between the theory and experiment, providing nearly exact agreement for YLD156 in chloroform.[42] It should be noted that experiments demonstrate that YLD156 has a 2-fold larger β_{HRS} than EZ-FTC; however, the DFT calculations (using the B3LYP functional) predict that β_{HRS} values of these two chromophores should be nearly the same. Figure 3 presents the experimental $\beta^{mol/sol}_{HRS}$ values of YLD156 and CLD-1 in the various solvents as a function of the *cmr* (see Supplemental Data). The figure demonstrates that the general trend of experimentally observed and theoretically predicted β_{HRS} increases with an increase in dielectric (or *cmr*) for the chromophores investigated here.

As described previously, a qualitative understanding of β is embodied in the TSM (eq 1.12). The TSM also provides a prediction of the variation in β with solvent, and has been shown to be accurate for relatively simple NLO chromophores.[12,43] According to the TSM the variation in $\beta^{mol/\varepsilon}_{zzz}(-2\omega;\omega,\omega)$ with solvent can arise from variation in the ground-excited state energy gap, differences between the permanent dipole moments in the ground and excited state, and changes in the transition dipole moments. To evaluate the accuracy of the TSM in predicting the solvent dependence of $\beta^{mol/\varepsilon}_{zzz}(-2\omega;\omega,\omega)$ evident in Figure 3, calculations were performed to explore the interaction between the dielectric dependent solvent reaction field and molecular parameters contained in the TSM. In these calculations the geometry of YLD156 was optimized with the reaction field turned on using B3LYP/6-31G*/PCM with default parameters provided in Gaussian03 for the solvents indicated (see Supporting Information). The dipole moment of the excited states was directly computed from the Gaussian09 codes. The results of these calculations are presented in Figure 4, where $\beta^{mol/\varepsilon}_{zzz}(-2\omega;\omega,\omega)$ is plotted versus cmr. For the interpretation of these results with measured β_{HRS}, one can use the approximation $\beta_{HRS} \approx (1/2)|\beta_{zzz}|$ for all frequencies and solvents, with this approximation being accurate to within about 3% for the molecules of interest. Figure 4 also illustrates that the TSM does accurately predict $\beta^{mol/\varepsilon}_{zzz}(-2\omega;\omega,\omega)$ in vacuum (*cmr* = 0). Furthermore, the TSM predicts that the solvent dependence of β_{zzz} for YLD156 should be small, with β_{zzz} *decreasing* with increasing *cmr*. Both of these predictions are in opposition to the experimental and theoretical results presented here. Solvent-induced changes in the energy and homogeneous line width associated with the lowest-energy absorption band can also affect β_{zzz} (eq 1.15). To investigate this effect, $\beta_{zzz}(0;0,0)$ was computed from the full calculation and then multiplied by $K_D(\omega,\gamma)$ as defined in eq 1.14. This approximate theory accounts for about half of the increase in $\beta_{zzz}(-2\omega;\omega,\omega)$ with solvent (see Figure 4). Variation in γ from 0 to 0.1 eV (or 0 to 800 cm^{-1}) was performed. Although this approximate theory also provides excellent agreement for the vacuum (*cmr* = 0) results, the theory did not improve the overall agreement with the more complete theory or increase $\beta_{zzz}(-2\omega;\omega,\omega)$ further. We would note that an inherent approximation in this approach is that the breadth of the absorption spectrum arises exclusively from homogeneous broadening. Given the absence of knowledge regarding the extent of inhomogeneous broadening in the systems investigated here, or how the homogeneous and inhomogeneous broadening varies as a function of solvent, this approximation provides only an estimation of the dependence of the HRS intensities on broadening.

Another prediction of the TSM is that β should depend on the bond length alternation (BLA), or the difference in length between the single and double bonds in the conjugated portion of the chromophore. Specifically, β is predicted to approach zero as the BLA goes to zero in the range $0 \leq$ BLA ≤ 0.05.[10,11,13,14,44,45]

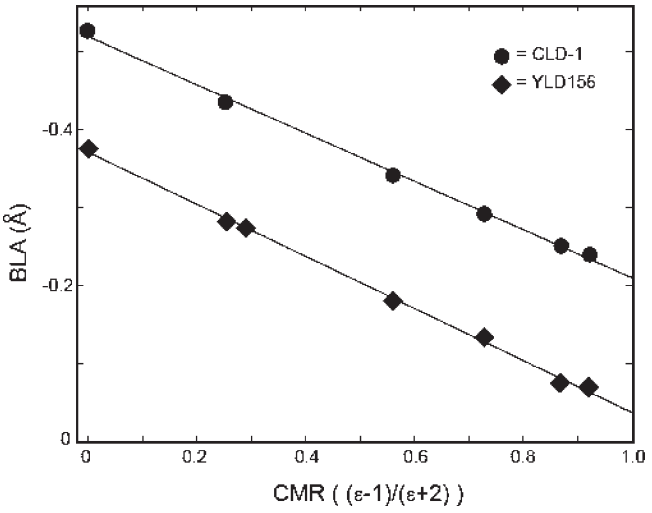

Figure 5. Calculated bond length alternation, based on the bond lengths (see Supporting Information), obtained from the solvent dependent geometry of each chromophore. The sum is computed as follows: bond length = $(1/5)\Sigma_{k=1}^{N=10}(-1)^k d_k$. The two curves differ by nearly a constant factor of 0.015 Å. The dashed lines represent a least-squares best fit linear lines to aid the eye.

Figure 5 presents the theoretically determined BLA of YLD156 and CLD-1 as a function of the *cmr*. The BLA was determined from the geometry-optimized structure in each solvent dielectric using the PCM model in Gaussian09. The BLA for CLD-1 is consistently about 0.015 Å larger because the nominally single bond (bond 5 in Scheme 1) in the isophorone ring contains more single-bond character than the analogous bond in the thiofuran ring of YLD156. The prediction of the TSM is that the β of CLD-1 should be markedly larger than that of YLD156 due to this difference in BLA since CLD-1 is further from the cyanine limit than YLD156. However, both theory and experiment show the two have almost identical hyperpolarizabilities (see Figure 3). Furthermore, Figures 3 and 4 show that the β of these molecules increases with *cmr*, yet BLA *decreases* with an increase in *cmr*. Finally, the BLA of YLD156 approaches zero as the dielectric becomes infinite (*cmr* = 1), where according to the TSM β should vanish. In contrast, the full theoretical treatment and the experimental results indicate that the molecular β is significantly larger in high dielectric solvents than in vacuum (see Figure 4). In summary, both experiment and theory demonstrate that for YLD156 and CLD-1, the TSM and BLA models are inadequate to explain the solvent-dependent β of these chromophores.

DISCUSSION

The results presented here demonstrate that the value of β for CLD-1 and YLD156 depends strongly on the dielectric constant of the surroundings. Figure 3 demonstrates that a roughly 10-fold increase in $\beta_{HRS}(-2\omega;\omega,\omega)$ is predicted to occur as the dielectric increases from vacuum ($\varepsilon = 0$) to solvents of moderate dielectric (e.g., acetonitrile for which $\varepsilon = 36$ or *cmr* = 0.92 at room temperature), and this prediction is consistent with experiment. One explanation for this behavior is that with an increased dielectric, the stability of the charge-transfer excited state is enhanced relative to the neutral ground state. This results in a decrease in the energy separation between these two states, and a corresponding increase in the charge-transfer character of the ground state. With an increase in the charge-transfer character of the ground state, the molecular β is enhanced. On the other hand, this explanation also requires that the charge-transfer absorption band shift to lower energy with an increase in the dielectric constant, yet Figure 2 demonstrates that the evolution in the absorption-band with a change in solvent is more complex. A shift to lower energy is indeed observed from vacuum to *cmr* $\leq$ 0.5, but further increases in dielectric result in a shift to higher energy. Therefore, where this theory would predict a *decrease* in $\beta_{HRS}(-2\omega;\omega,\omega)$ at elevated dielectric instead of the increase observed here. This discrepancy suggests that assigning the origin of the molecular hyperpolarizability to the lowest-energy state is an oversimplification for these chromophores, and that other states must be considered in order to fully capture the solvent-dependence of $\beta_{HRS}(-2\omega;\omega,\omega)$. This conclusion is supported by the ability of the full-theoretical treatment to reproduce the evolution in $\beta_{HRS}(-2\omega;\omega,\omega)$ as illustrated in Figure 3, a treatment in which contributions from multiple excited states are included.

The inability of this single-state perspective to reproduce the solvent dependence of $\beta_{HRS}(-2\omega;\omega,\omega)$ is highlighted by the inability of the TSM to explain the solvent dependence observed here (Figures 4 and 5). Recall, the TSM restricts the sum in eq 1.9 to terms only involving the lowest-energy excited state. In this limit, the variation in $\beta_{HRS}(-2\omega;\omega,\omega)$ with dielectric depends exclusively on molecular parameters derived from the ground and lowest excited state (transition dipole moment, permanent dipole moments for the ground and excited state, and the ground-to-excited state transition energy). In the results presented above, these parameters were determined and used to predict the variation in $\beta_{HRS}(-2\omega;\omega,\omega)$ with dielectric. We found that not only was the TSM incapable of reproducing the evolution in $\beta_{HRS}(-2\omega;\omega,\omega)$, it actually predicts behavior that is opposite to what is observed. Figure 5 presents a test of the central prediction of the TSM: as the BLA approaches zero, $\beta_{HRS}(-2\omega;\omega,\omega)$ should also approach zero. For the chromophores studied here, the direct opposite of this prediction occurs. Although the TSM has been applied with some success to less complicated NLO chromophores,[8,22,46−51] the studies presented here demonstrate that the applicability of the TSM to more complicated chromophores is questionable at best, and that any attempt to model the solvent-dependence of $\beta_{HRS}(-2\omega;\omega,\omega)$ for these systems requires a full theoretical treatment in which the contribution from multiple excited states is included.

While reasonable agreement between experiment and theory regarding the effect of solvent on molecular hyperpolarizabilities was achieved, quantitative differences remain to be explained. Specifically, the theoretical treatment employed here predicts that $\beta_{HRS}(-2\omega;\omega,\omega)$ for CLD-1 and YLD156 should be close, yet the experimental values for YLD156 are elevated relative to CLD-1 (Figure 3). In addition, theoretical prediction of $\beta_{HRS}(-2\omega;\omega,\omega)$ for EZ-FTC in chloroform (the reference employed in this study) is roughly 2-fold greater than the experimentally measured value. One explanation for these discrepancies lies in the nature of the functional employed. Recently, Truhlar[52] and co-workers have shown that modification of the functional employed can have a significant effect on predicted hyperpolarizabilities. In addition, accurate modeling of the differences in homogeneous linewidths between chromophores is also required to accurately predict $\beta_{HRS}(-2\omega;\omega,\omega)$. In summary, quantitative agreement between experiment and theory will require improvement in functionals combined with a determination of the spectroscopic parameters relevant to $\beta_{HRS}(-2\omega;\omega,\omega)$.

Finally, the results presented here highlight a new direction by which to obtain enhanced performance in NLO devices employing these chromophores. The electro-optical coefficient is dependent on the product of β_{zzz}, number density, N, and the extent of acentric order, $\langle\cos^3\theta\rangle$, where θ is the angle between the permanent dipole moment of the chromophore and the vector describing the orientation of the aligning potential. Typical concentrations of chromophores in guest−polymer host systems are 20 wt % in chromophore relative to the polymer, and this represents a maximum in *N*. Recent studies of chromophore acentric order suggest in guest−host systems the extent of order is modest with $\langle\cos^3\theta\rangle \leq 0.15$.[8,49−51] Increases in acentric order may be achieved by increasing the alignment potential or reducing the orientational dimensionality of the host; both are avenues that present significant barriers with respect to materials development and device construction. In contrast, the studies presented here suggest that significant gains in β_{zzz} can be readily achieved by tuning the dielectric of the host. It should be noted that an increase in dielectric constant can limit switching speeds due to increased capacitance. However, amorphous polycarbonate is a common polymer host due to the advantageous thermal properties of this material, and the dielectric constant of this polymer is modest ($\varepsilon \approx 4$). The results presented here suggest that by employing polymer hosts with increased dielectric appreciable increases in electro-optic activity can be achieved.

■ ASSOCIATED CONTENT

Supporting Information. Tables of numerical values for the experimental and theoretical data presented in the figures. This material is available free of charge via the Internet at http://pubs.acs.org.

■ AUTHOR INFORMATION

Corresponding Author

*E-mail: (B.H.R.) robinson@chem.washington.edu; (P.J.R.) preid@chem.washington.edu.

■ ACKNOWLEDGMENT

The authors gratefully acknowledge the financial support of this work provided by the National Science Foundation (Grants DMR-0120967 and DMR-0551020).

■ REFERENCES

(1) Prasad, P. N.; Williams, D. J. *Introduction to Nonlinear Optical Effects in Molecules and Polymers*: Wiley-Interscience: New York, 1990.

(2) Dalton, L. R.; Lao, D.; Olbricht, B. C.; Benight, S.; Bale, D. H.; Davies, J. A.; Ewy, T.; Hammond, S. R.; Sullivan, P. A. *Opt. Mater.* **2010**, *32*, 658.

(3) Sullivan, P. A.; Dalton, L. R. *Acc. Chem. Res.* **2010**, *43*, 10.

(4) Pereverzev, Y. V.; Gunnerson, K. N.; Prezhdo, O. V.; Sullivan, P. A.; Liao, Y.; Olbricht, B. C.; Akelaitis, A. J. P.; Jen, A. K. Y.; Dalton, L. R. *J. Phys. Chem. C* **2008**, *112*, 4355.

(5) Kim, T. D.; Kang, J. W.; Luo, J. D.; Jang, S. H.; Ka, J. W.; Tucker, N.; Benedict, J. B.; Dalton, L. R.; Gray, T.; Overney, R. M.; Park, D. H.; Herman, W. N.; Jen, A. K. Y. *J. Am. Chem. Soc.* **2007**, *129*, 488.

(6) Kim, T. D.; Luo, J. D.; Cheng, Y. J.; Shi, Z. W.; Hau, S.; Jang, S. H.; Zhou, X. H.; Tian, Y.; Polishak, B.; Huang, S.; Ma, H.; Dalton, L. R.; Jen, A. K. Y. *J. Phys. Chem. C* **2008**, *112*, 8091.

(7) Ding, R.; Baehr-Jones, T.; Liu, Y.; Bojko, R.; Witzens, J.; Huang, S.; Luo, J.; Benight, S.; Sullivan, P.; Fedeli, J. M.; Fournier, M.; Dalton, L.; Jen, A.; Hochberg, M. *Opt. Express* **2010**, *18*, 15618.

(8) Sullivan, P. A.; Rommel, H. L.; Takimoto, Y.; Hammond, S. R.; Bale, D. H.; Olbricht, B. C.; Liao, Y.; Rehr, J.; Eichinger, B. E.; Jen, A. K. Y.; Reid, P. J.; Dalton, L. R.; Robinson, B. H. *J. Phys. Chem. B* **2009**, *113*, 15581.

(9) Reichardt, C. *Solvents and Solvent Effects in Organic Chemistry*, 3rd ed.; Wiley-VCH: New York, 2003.

(10) Marder, S. R.; Cheng, L. T.; Tiemann, B. G.; Friedli, A. C.; Blanchard-Desce, M.; Perry, J. W.; Skindhoej, J. *Science* **1994**, *263*, 511.

(11) Marder, S. R.; Perry, J. W.; Bourhill, G.; Gorman, C. B.; Tiemann, B. G.; Mansour, K. *Science* **1993**, *261*, 186.

(12) Bourhill, G.; Bredas, J.-L.; Cheng, L.-T.; Marder, S. R.; Meyers, F.; Perry, J. W.; Tiemann, B. G. *J. Am. Chem. Soc.* **1994**, *116*, 2619.

(13) Marder, S. R.; Perry, J. W.; Tiemann, B. G.; Gorman, C. B.; Gilmour, S.; Biddle, S. L.; Bourhill, G. *J. Am. Chem. Soc.* **1993**, *115*, 2524.

(14) Gorman, C. B.; Marder, S. R. *Chem. Mater.* **1995**, *7*, 215.

(15) Huyskens, F. L.; Huyskens, P. L.; Persoons, A. P. *J. Chem. Phys.* **1998**, *108*, 8161.

(16) Hsu, C.-C.; Liu, S.; Wang, C. C.; Wang, C. H. *J. Chem. Phys.* **2001**, *114*, 7103.

(17) Shoute, L. C. T.; Helburn, R.; Kelley, A. M. *J. Phys. Chem. A* **2007**, *111*, 1251.

(18) Shoute, L. C. T.; Woo, H. Y.; Vak, D.; Bazan, G. C.; Kelley, A. M. *J. Chem. Phys.* **2006**, *125*, 054506.

(19) Brown, E. C.; Marks, T. J.; Ratner, M. A. *J. Phys. Chem. B* **2008**, *112*, 44.

(20) Smith, G. J.; Middleton, A. P.; Clarke, D. J.; Teshome, A.; Kay, A. J.; Bhuiyan, M. D. H.; Asselberghs, I.; Clays, K. *Opt. Mater.* **2010**, *32*, 1237.

(21) Moran, A. M.; Egolf, D. S.; Blanchard-Desce, M.; Kelley, A. M. *J. Chem. Phys.* **2002**, *116*, 2542.

(22) Zuliani, P.; Delzoppo, M.; Castiglioni, C.; Zerbi, G.; Marder, S. R.; Perry, J. W. *J. Chem. Phys.* **1995**, *103*, 9935.

(23) Oudar, J. L. *J. Chem. Phys.* **1977**, *67*, 446.

(24) Oudar, J. L.; Chemla, D. S. *J. Chem. Phys.* **1977**, *66*, 2664.

(25) Murugan, N. A.; Aagren, H. *J. Phys. Chem. A* **2009**, *113*, 2572.

(26) Li, H.-P.; Han, K.; Tang, G.; Li, M.-X.; Shen, X.-P.; Huang, Z.-M. *Mol. Phys.* **2009**, *107*, 1597.

(27) Mendes, P. J.; Silva, T. J. L.; Carvalho, A. J. P.; Ramalho, J. P. P. *J. Mol. Struct.: Theochem* **2010**, *946*, 33.

(28) Sainudeen, Z.; Ray, P. C. *J. Phys. Chem. A* **2005**, *109*, 9095.

(29) Perpete, E. A.; Jacquemin, D. *Int. J. Quantum Chem.* **2007**, *107*, 2066.

(30) Corozzi, A.; Mennucci, B.; Cammi, R.; Tomasi, J. *J. Phys. Chem. A* **2009**, *113*, 14774.

(31) Zhang, C.; Dalton, L. R.; Oh, M.-C.; Zhang, H.; Steier, W. H. *Chem. Mater.* **2001**, *13*, 3043.

(32) Liao, Y.; Anderson, C. A.; Sullivan, P. A.; Akelaitis, A. J. P.; Robinson, B. H.; Dalton, L. R. *Chem. Mater.* **2006**, *18*, 1062.

(33) Singer, K. D.; Kuzyk, M. G.; Sohn, J. E. *J. Opt. Soc. Am. B: Opt. Phys.* **1987**, *4*, 968.

(34) Canfield, B. K.; Kuzyk, M. G.; Hightower, S. E.; Li, A. D. Q. *J. Opt. Soc. Am. B* **2005**, *22*, 723.

(35) Rice, J. E.; Amos, R. D.; Colwell, S. M.; Handy, N. C.; Sanz, J. *J. Chem. Phys.* **1990**, *93*, 8828.

(36) Orr, B. J.; Ward, J. F. *Mol. Phys.* **1971**, *20*, 513.

(37) Gaussian Quantum Chemistry Codes, Gaussian, 2009.

(38) DMOL^3; Accelrys Corp.: San Diego, CA, 2002.

(39) Davies, J. A.; Elangovan, A.; Sullivan, P. A.; Olbricht, B. C.; Bale, D. H.; Ewy, T. R.; Isborn, C. M.; Eichinger, B. E.; Robinson, B. H.; Reid, P. J.; Li, X.; Dalton, L. R. *J. Am. Chem. Soc.* **2008**, *130*, 10565.

(40) Cyvin, S. J.; Rauch, J. E.; Decius, J. C. *J. Chem. Phys.* **1965**, *43*, 4083.

(41) Kinnibrugh, T.; Bhattacharjee, S.; Sullivan, P.; Isborn, C.; Robinson, B. H.; Eichinger, B. E. *J. Phys. Chem. B* **2006**, *110*, 13512.

(42) Firestone, K. A.; Lao, D. B.; Casmier, D. M.; Clot, O.; Dalton, L. R.; Reid, P. J. *Proc. SPIE—Int. Soc. Opt. Eng.* **2005**, *5935*, 59350P/1.

(43) Marder, S. R.; Gorman, C. B.; Meyers, F.; Perry, J. W.; Bourhill, G.; Bredas, J.-L.; Pierce, B. M. *Science* **1994**, *265*, 632.
(44) Barzoukas, M.; Runser, C.; Fort, A.; Blanchard-Desce, M. *Chem. Phys. Lett.* **1996**, *257*, 531.
(45) Blanchard-Desce, M.; Barzoukas, M. *J. Opt. Soc. Am. B* **1998**, *15*, 302.
(46) Woodford, J. N.; Pauley, M. A.; Wang, C. H. *J. Phys. Chem. A* **1997**, *101*, 1989.
(47) Kodaira, T.; Watanabe, A.; Ito, O.; Matsuda, M.; Clays, K.; Persoons, A. *J. Chem. Soc., Faraday Trans.* **1997**, *93*, 3039.
(48) Thompson, W. H.; Blanchard-Desce, M.; Alain, V.; Muller, J.; Fort, A.; Barzoukas, M.; Hynes, J. T. *J. Phys. Chem. A* **1999**, *103*, 3766.
(49) Benight, S. J.; Johnson, L. E.; Barnes, R.; Olbricht, B. C.; Bale, D. H.; Reid, P. J.; Eichinger, B. E.; Dalton, L. R.; Sullivan, P. A.; Robinson, B. H. *J. Phys. Chem. B* **2010**, *114*, 11949.
(50) Sullivan, P. A.; Rommel, H.; Liao, Y.; Olbricht, B. C.; Akelaitis, A. J. P.; Firestone, K. A.; Kang, J.-W.; Luo, J.; Davies, J. A.; Choi, D. H.; Eichinger, B. E.; Reid, P. J.; Chen, A.; Jen, A. K. Y.; Robinson, B. H.; Dalton, L. R. *J. Am. Chem. Soc.* **2007**, *129*, 7523.
(51) Olbricht, B. C.; Sullivan, P. A.; Dennis, P. C.; Hurst, J. T.; Johnson, L. E.; Benight, S. J.; Davies, J.; Chen, A. T.; Eichinger, B. E.; Reid, P. J.; Dalton, L. D.; Robinson, B. H. *J. Phys. Chem. B* **2011**, *115*, 231.
(52) Marenich, A. V.; Cramer, C. J.; Truhlar, D. G. *J. Chem. Theor. Comp.* **2010**, *6*, 2829.